Supramolecular Environment-Dependent Electronic Properties of Metal-Organic Interfaces.

ARTICLE *in* THE JOURNAL OF PHYSICAL CHEMISTRY C · FEBRUARY 2012

Impact Factor: 4.77 · DOI: 10.1021/jp211749g

THE JOURNAL OF PHYSICAL CHEMISTRY C

Article

pubs.acs.org/JPCC

Supramolecular Environment-Dependent Electronic Properties of Metal–Organic Interfaces.

Afaf El-Sayed,[†] Duncan J. Mowbray,[‡] Juan M. García-Lastra,[§] Celia Rogero,[†,‡] Elizabeth Goiri,[‡] Patrizia Borghetti,[‡] Ayse Turak,[∥] Bryan P. Doyle,[⊥] Martina Dell'Angela,[#] Luca Floreano,[#] Yutaka Wakayama,[▽] Angel Rubio,[§] J. Enrique Ortega,[†,‡,○] and Dimas G. de Oteyza*[,†,◆]

[†]Centro de Física de Materiales (CSIC-UPV/EHU)-Materials Physics Center (MPC), Paseo Manuel Lardizabal 5, 20018 San Sebastián, Spain

[‡]Donostia International Physics Center (DIPC), Paseo Manuel Lardizabal 4, San Sebastián, Spain

[§]Nano-Bio Spectroscopy group and European Theoretical Spectroscopy Facility, Departamento Fisica de Materiales UPV/EHU, San Sebastián, Spain

[∥]Max-Planck Institute for Metal Research, Heisenbergstr 3, 70569 Stuttgart, Germany

[⊥]Department of Physics, University of Johannesburg, Auckland Park, Johannesburg, South Africa

[#]CNR-IOM, Laboratorio Nazionale TASC, Basovizza SS-14 Km. 163.5, I-34149, Trieste, Italy

[▽]Advanced Electronic Materials Center, National Institute for Materials Science, 1-1 Namiki, Tsukuba 305-0044, Japan

[○]Departamento de Fisica Aplicada I, UPV/EHU, 20018 San Sebastián, Spain

[◆]Department of Physics, University of California at Berkeley, Berkeley, California, United States

ABSTRACT: Model donor–acceptor assemblies at metal–organic interfaces, namely, fluorinated copper-phthalocyanines (F_{16}CuPC) and pentacene (PEN) assemblies on the Au(111) surface, have been the focus of the present study. A full picture of the crystallographic and electronic structure of PEN and F_{16}CuPC monolayers as well as of their 1:1 binary mixture on the Au(111) surface has been explored by means of a variety of surface-sensitive techniques, providing important information on the intermolecular and molecule–substrate interactions governing the self-assembly process. A long-range ordered donor–acceptor network is observed for the mixture as a result of the greatly enhanced intermolecular interaction via C–F···H–C hydrogen bonds. Interestingly, the new supramolecular structure involves changes in the electronic structure of the molecular components. In particular, the strongest changes are observed at the C and F atoms of the F_{16}CuPc, as opposed to the F_{16}CuPc N, Cu, or PEN C atoms. With the aid of theoretical calculations, such effects are found to be at least partially related to an upward shift in energy of the F_{16}CuPc molecular orbitals, concomitant with a molecule-to-metal charge donation, not from the HOMO, but deeper lying orbitals.

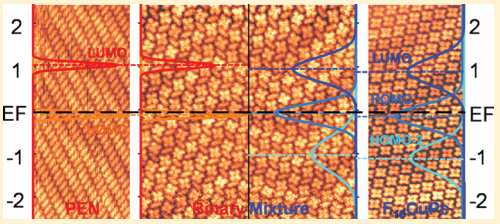

INTRODUCTION

Organic electronics has become an enormously promising field of technology due to the prospect of size reduction offered by molecular-level control of the relevant material properties. However, many challenges still have to be overcome before this technology becomes mature and commercially competitive, requiring first a thorough understanding of the basic science involved in the operation of organic electronic devices and the physics of organic semiconductors.[1−3] Of particular interest and relevance for the performance of organic electronics, we find the various interfaces present in the devices, where such crucial processes such as, for example, charge injection or exciton separation take place. Pursuing a better understanding of such interfaces, many studies are being devoted to the investigation of model systems like donor–acceptor assemblies on various substrates.[4−13] Combination of different molecules on a surface provides a perfect platform to study interfacial phenomena, as both organic–organic (e.g., donor–acceptor) interfaces between the neighboring molecules and organic–inorganic (in case of inorganic substrates) interfaces are simultaneously present in a 2D system easily accessible by a large variety of experimental techniques, while keeping its complexity low enough to be accessible and therefore profit from first principle calculations. Besides, an appropriate choice of substrate, molecules and their functionalities, allows control over the relevant molecule–substrate and intermolecular interactions.[14−17]

Fluorinated copper-phthalocyanines (F_{16}CuPC, acceptor) and pentacene (PEN, donor) molecules are well-known, extensively studied, and widely used materials due to their successful integration and high performance in organic electronic devices.[18] Hence, many studies have been performed

Received: December 6, 2011
Revised: January 23, 2012
Published: January 24, 2012

on their combination at various interfaces and architectures.[10−12,19] Here we present a comprehensive study on F_{16}CuPc and PEN mixed monolayers on Au(111). By means of comparison with the corresponding single component layers, the dependence on the supramolecular environment of the electronic structure of F_{16}CuPc and PEN is investigated. A variety of highly surface-sensitive techniques such as scanning tunneling microscopy (STM), X-ray photoemission spectroscopy (XPS), and ultraviolet valence band photoemission (UPS), in combination with density functional theory (DFT) calculations, have been used.

RESULTS AND DISCUSSION

The monolayer structures of single-component and binary layers as obtained from STM measurements are summarized in Figure 1.[12] All of the layers form highly crystalline films with

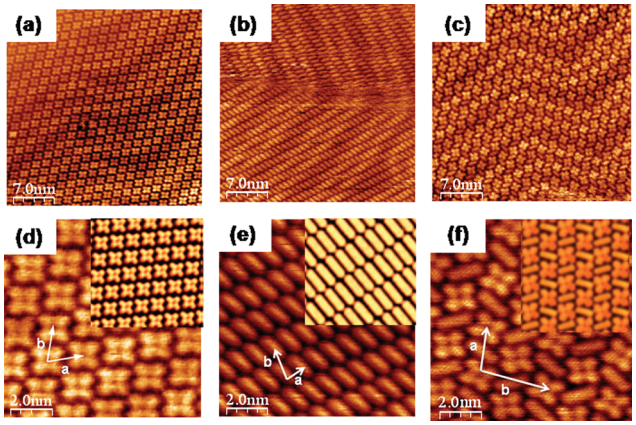

Figure 1. STM images for F_{16}CuPc and PEN monolayers and their 1:1 mixture on the Au(111) surface. (a−c) Respective large scale images. (d−f) Respective small scale images. The insets represents the DFT calculations.

epitaxial relations to the substrate, evidenced by the discrete number of rotational domains. The arrangement of F_{16}CuPc on Au(111) is characterized by a unique oblique unit cell of parameters listed in Table 1 and has been described in detail in

Table 1. Unit Cell Parameters Obtained by STM (High Bold Values) and by DFT Calculations (Low Values)

	a (Å)	b (Å)	γ (°)
F_{16}CuPc	**15.1 ± 0.8**	**14.5 ± 0.8**	**75 ± 3**
	15.3	14.4	79.1
PEN	**6 ± 1**	**15 ± 1**	**75 ± 3**
	6.7	15.3	79.1
binary layer (1:1)	**22.5 ± 2**	**28.5 ± 2**	**90 ± 3**
	23.1	30.0	90

previous work.[20] In turn, pentacene has been shown to present polymorphism at the Au(111) interface, and the structure observed in Figure 1 with its associated unit cell (see Table 1 for parameters) corresponds to only one of the possible arrangements.[21]

The optimized molecular arrangement of the different layers has been further modeled with DFT calculations, resulting in an excellent agreement with the experimental data. This is evidenced by comparison of the simulated STM images resulting from the calculated overlayers on Au(111) (shown as insets in Figure 1) and the experimental ones. Calculated and experimental parameters are included in Table 1. Additional important information obtained from the calculations is the respective molecule−substrate interaction strength, which plays a key role in the electronic properties of metal−organic interfaces. Our results predict adsorption energy per molecule in the respective layers of 1.955 eV for F_{16}CuPc and 1.41 eV for PEN. Calculations were performed with the local density approximation (LDA) as well as with van der Waals (vdW) functionals. The latter includes long-range vdW interactions, which have been shown to dominate the PEN-Au(111) interactions.[22] The adsorption energy values given above are obtained from vdW calculations but showed only minor variations (<10%) with LDA.

Co-deposition of these two molecules in a 1:1 ratio leads to a highly crystalline mixed layer, as shown in Figure 1. The unit cell, with parameters outlined in Table 1, with vectors aligned along the high symmetry Au(111) surface directions and comprising four molecules, is described in detail in a previous work.[12] In this mixed layer, each molecule is surrounded by the opposite species (Figure 1). Such an arrangement is adopted so as to maximize the C−F···H−C interactions between F_{16}CuPc and PEN. The resulting layer is thus characterized by an enhanced stability that makes it indeed easier to image by STM than the single component films. This is confirmed with the calculations, which conclude an enhanced stabilization energy of the mixed layer by 0.77 eV per F_{16}CuPc-PEN pair. The number of F···H atom pairs at distances under 3.1 Å is 10, giving an average C−F···H−C bond strength of 77 meV.

Of special interest is how the new supramolecular environment in a donor−acceptor network affects the electronic structure of the individual molecules and thereby its potential functionality. In this frame, XPS spectra of the various atomic species measured on the different molecular layers provide important information. Such measurements are depicted in Figure 2.[23−25] Comparison of the spectra of single-component and binary layers evidence several differences, illustrated by lines connecting the peak positions in the different spectra.

In the case of PEN, the analysis is complicated by the shifts present even in single-component PEN layers as a function of coverage. We observe these to be of up to 0.1 eV toward higher binding energy as we pass from 0.2 to 1 ML. (See Figure 2b.) Polymorphism is very pronounced for pentacene on Au(111), with nine different structures reported, some of them as a function of layer coverage.[21] Such variation changes the screening from neighboring molecules[26] as well as the relative position of PEN atoms with respect to the underlying gold, which might in turn modify hybridization or also molecule−substrate distances and thereby screening from the substrate. In addition, the local work function can vary as a function of coverage and thereby change the binding energy of electronic levels, in a similar way to that observed for CuPc on Au(111).[27] All of the above can explain the coverage dependence in PEN XPS spectra but makes a comparison with the mixed layer spectrum more difficult, which happens to coincide with the 0.5 ML spectrum.

Moving our attention now to F_{16}CuPc, stronger differences are observed. In particular we observe shifts of ∼0.1 eV toward higher binding energies of the C−C (C2), C−N (C1), and N1s components, whereas larger shifts of ∼0.2 eV are observed for the C−F (C3,C4) and F1s components associated with the outer molecular atoms (Figure 2c). Asymmetries between F_{16}CuPc and PEN in the magnitude of the core-level shift may

dx.doi.org/10.1021/jp211749g | J. Phys. Chem. C 2012, 116, 4780−4785

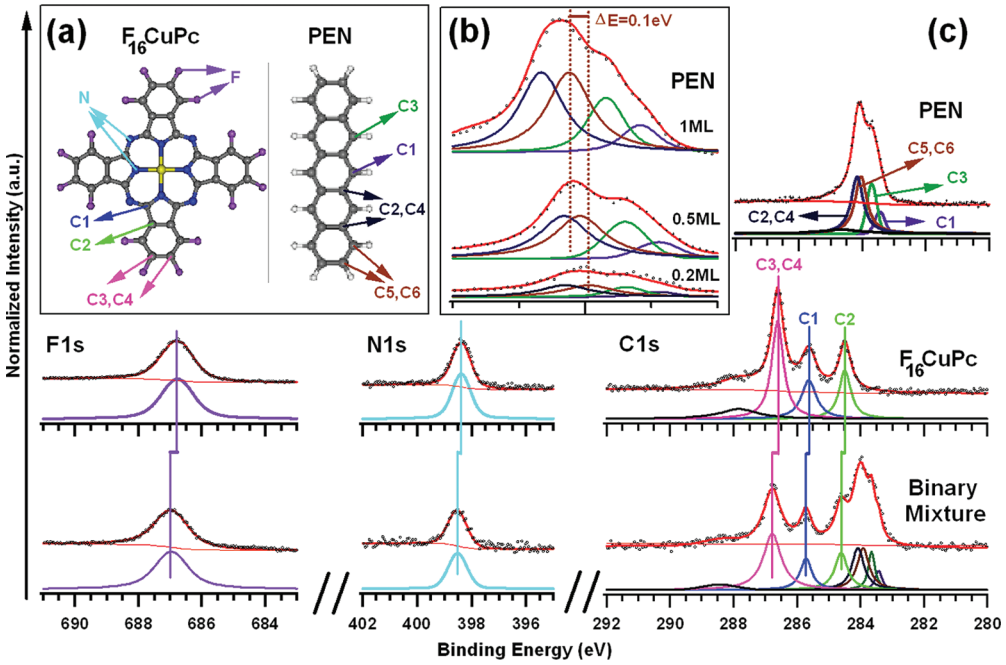

Figure 2. (a) Chemical structure of PEN and F_{16}CuPc molecules. (b) PEN C1s shift as a function of coverage. As a guide to the eye, vertical lines mark the initial and final position of one of the peaks. (c) C1s, N1s, and F1s core-level photoemission spectra for the single component molecular layers as well as for their binary mixture on Au(111). All peaks were fitted with their corresponding shakeup satellites, if observed, caused by a kinetic energy loss of the photoelectrons upon simultaneous excitation of $\pi-\pi^*$, HOMO−LUMO transitions.

reflect a more significant charge transfer from F_{16}CuPc to the substrate, as discussed below.

Next, we analyze the changes in the valence and conduction bands of our system. Figure 3a depicts the projected density of states for the highest occupied molecular level (HOMO), HOMO-2, and the lowest unoccupied molecular level (LUMO). Whereas no changes are observed for the PEN, all F_{16}CuPc molecular orbitals move up in energy by ∼0.07 eV in the binary layers. As a consequence, the charge transfer from F_{16}CuPc to Au(111) is increased from 0.32 to 0.44 electrons per molecule, whereas the charge transfer between PEN and Au(111) is negligibly small regardless of the layer structure.

Interestingly, the increased charge transfer does not stem from the F_{16}CuPc HOMO, as would initially be expected. In that case, the HOMO being located mainly in the central part of the molecule, the Cu and N core levels (and their corresponding XPS spectra), would be most strongly affected, as was indeed observed in the very similar system combining F_{16}CuPc and diindenoperylene (DIP) on Au(111).[28] Instead, the charge transfer stems mainly from deeper lying molecular orbitals, in particular, from the quasi-degenerate HOMO-2, HOMO-3, and HOMO-4 that are ∼1 eV lower in energy (Figure 3a) and show a significant density on the outer parts of the molecule. This is due to the fact that whereas the HOMO moves up in energy, it simultaneously narrows (as a result of a decreased hybridization). Both effects counteract and finally lead to a virtually unchanged charge flow involving the HOMO. Instead, the deeper lying HOMO-2 to HOMO-4 do both move up in energy and broaden, by which their high-energy tails cross the Fermi energy and lead to the charge transfer. Charge transfer from deeper-lying orbitals was previously found also for F4-TCNQ on Cu(111)[29] and stresses the importance of taking into account molecular orbitals beyond the HOMO and LUMO, which capture most of researchers' attention, to understand the physical−chemical processes taking place at metal−organic interfaces.

Further proof of this scenario is obtained from UPS measurements presented in Figure 3b with valence band spectra of F_{16}CuPC and binary layers. Whereas the lower lying HOMO-2 is not observed, shaded by the strong onset of the Au 5d bands, we do measure the HOMO level. Not only is the position in relatively good agreement with the theoretical calculations[30−33] but also we observe a similar upward shift in energy as well as a narrowing for the mixed layer.[34]

The spatial distribution of the charge transfer is best visualized by mapping the electron density changes on the molecules, as shown in Figure 4. Such a picture reflects the negligible charge transfer on PEN, the largest contribution to charge transfer on F_{16}CuPc arising from the inner molecular region (where the HOMO is located), and most importantly, the main charge transfer differences upon growth of mixed layers on the outer regions of the molecule, in perfect agreement with the XPS findings.

■ CONCLUSIONS

The experimentally observed and theoretically calculated results provide a coherent and comprehensive picture of the crystalline and electronic structures of single component PEN and F_{16}CuPc layers as well as of their binary donor−acceptor mixture on Au(111). The results show small but unambiguous changes in the electronic properties of the molecules depending on their supramolecular environment. These electronic changes mainly affect the F_{16}CuPc. When immersed in the binary mixture with greatly enhanced intermolecular interactions via C−F···H−C bonds, its molecular orbitals move up in energy, leading to an increased charge transfer from molecules to substrate. Interestingly, the latter does not stem from the molecular HOMO but from deeper lying orbitals. These results stress the importance of the molecular orbitals beyond the

dx.doi.org/10.1021/jp211749g | J. Phys. Chem. C 2012, 116, 4780−4785

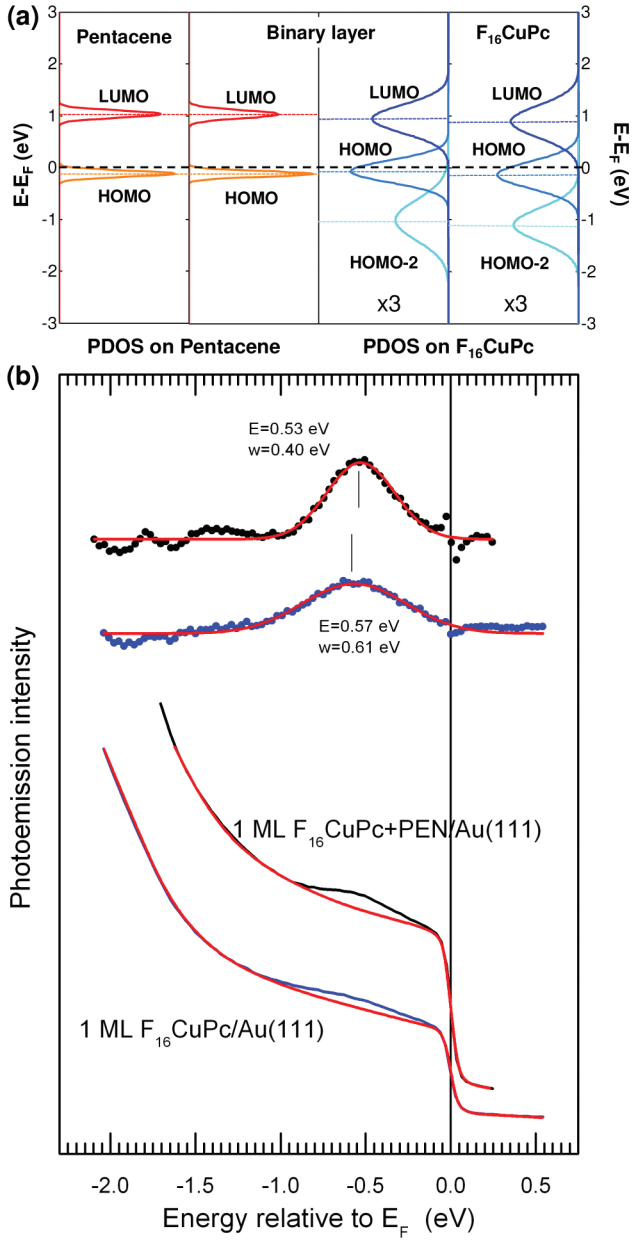

Figure 3. (a) Projected density of states on the HOMO and LUMO of F_{16}CuPc and PEN for the single component and binary layers. Notice that the F_{16}CuPc PDOS is scaled by a factor of 3 with respect to the PEN one. (b) HOMO level of the single component F_{16}CuPc and binary layers on Au(111) surface as observed by the ARPES measurements. Below are the curves as recorded, and above are the curves upon substrate normalization and fitting.

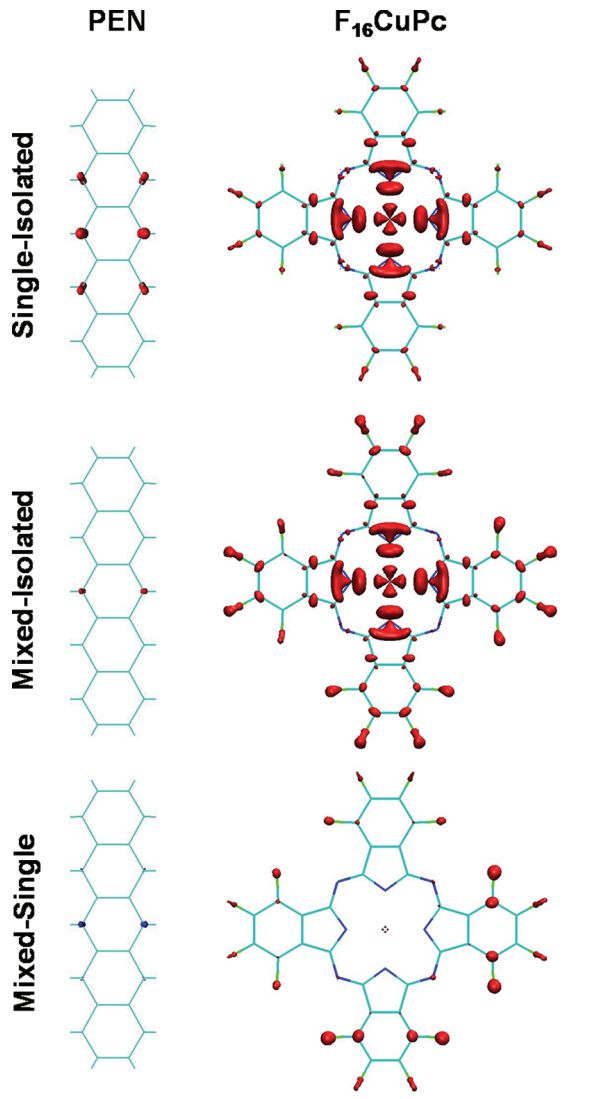

Figure 4. Difference in the electronic densities with respect to the isolated molecules for F_{16}CuPc and PEN in the single-component and binary layers. For comparison purposes, the difference in the electronic densities between the single and mixed layers is also represented in the bottom panel. The represented isosurfaces in red (blue) contain the points where the electronic density lessens (increases). In the case of PEN, the changes are magnified four-fold with respect to the F_{16}CuPc to be visible.

frontier levels HOMO and LUMO, which commonly capture the most attention. We hereby provide important new input on the still poorly understood interplay between molecule–molecule and molecule–substrate interactions, which might eventually allow us to control and even design a priori functional donor–acceptor mixtures with optimized properties.

METHODS

The Au(111) surface was prepared by standard sputtering ($E \approx$ 600–1000 eV) at a pressure of $\sim 1 \times 10^{-5}$ mbar of Ar^+ for 20–30 min, followed by annealing cycles ($T \approx 400$ °C) for 15–20 min. The molecular layers were prepared by the deposition from a resistively heated Knudsen-cell onto the clean Au substrate held at room temperature. All measurements were performed at room temperature under ultrahigh vacuum (UHV) conditions. The STM experiments have been carried out in a commercial JEOL system in constant current mode and with chemically etched tungsten tips. Data analysis was performed with the freeware WSxM.[35] The XPS spectra have been measured at the ALOISA beamline of the ELETTRA synchrotron in Trieste, Italy. Careful thickness calibration was performed to avoid multilayer deposition in both pure and mixed films, as this would lead to core-level shifts associated with the different molecular environment and modified core-hole screening from the substrate. This was corroborated by use of a calibrated quartz crystal microbalance as well as by detailed analysis of the relative core-level peak intensities. The N 1s and C 1s spectra have been taken at a photon energy of 520 eV with an overall energy resolution of 160 meV, whereas the F 1s peak

dx.doi.org/10.1021/jp211749g | J. Phys. Chem. C 2012, 116, 4780–4785

has been measured at 820 eV with a resolution of 340 meV. In both cases, the binding energy scale has been calibrated to that of the Au 4f bulk peak at 84 eV.[36] Potential beam damage on the films was discarded by checking the reproducibility of spectra after irradiation times well above those of typical measurements. UPS experiments were carried out at the Apple PGM beamline of the Synchrotron Radiation Center (SRC) in Stoughton, WI. We used a hemispherical Scienta SES200 spectrometer with energy resolution set to 25 meV and p-polarized light. Spectra in Figure 3b correspond to the integrated intensity recorded at the channelplate (7 deg. acceptance).

DFT calculations have been performed using the real-space projector-augmented wave function GPAW code,[37,38] within both the LDA[39] and a self-consistent van der Waals approximation[40,41] for the exchange-correlation functional, with a grid spacing of 0.2 Å. An electronic temperature of $k_BT \approx 0.1$ eV was employed to obtain the occupation of the Kohn−Sham orbitals, with all energies extrapolated to $T = 0$ K. Monolayers of PEN, F_{16}CuPc, and the 1:1 mixture (F_{16}CuPc + PEN) have been structurally optimized until a maximum force below 0.05 eV/Å was obtained in vacuum and adsorbed on the Au(111) surface, while keeping the coordinates of the metal slab fixed. The lattice parameters, shown in Table 1, are those commensurate with the experimental bulk lattice parameter of Au, $a \approx 4.08$ Å, which are nearest the periodicity of the monolayer on the surface as observed by STM.

AUTHOR INFORMATION

Corresponding Author

*E-mail: dgoteyza@berkeley.edu.

Notes

The authors declare no competing financial interest.

ACKNOWLEDGMENTS

This work was supported by the Spanish MICINN (MAT2010-21156-C03-01, C03-03, PIB2010US-00652) and the Basque Government (IT-257-07). The SRC is funded by the National Science Foundation (award no. DMR-0084402). B.P.D. thanks the ICTP (Trieste) for travel funding. The research leading to these results has received funding from the European Community's Seventh Framework Programme (FP7/2007-2013) under grant agreement no. 226716. The research leading to these results has received funding from the European Community's Seventh Framework Programme (FP7/2007-2013) through the Integrated Infrastructure Initiative "European Light Sources Activities − Synchrotrons and Free Electron Lasers" (grant agreement no. 226716).

REFERENCES

(1) Horowitz, G. *J. Mater. Res.* **2004**, *19*, 1946−1962.
(2) Brütting, W. *Physics of Organic Semiconductors*; Wiley-VCH Verlag: Weinheim, Germany, 2005.
(3) Klauk, H. *Organic Electronics: Materials, Manufacturing and Applications*; Wiley-VCH: Weinheim, Germany, 2006.
(4) Otero, R.; Ecija, D.; Fernandez, G.; Gallego, J. M.; Sanchez, L.; Martin, N.; Miranda, R. *Nano Lett.* **2007**, *7*, 2602−2607.
(5) Gonzalez-Lakunza, N.; Fernandez-Torrente, I.; Franke, K. J.; Lorente, N.; Arnau, A.; Pascual, J. I. *Phys. Rev. Lett.* **2008**, *100*, 156805-1−156805-4.
(6) Canas-Ventura, M. E.; Xiao, W.; Wasserfallen, D.; Mullen, K.; Brune, H.; Barth, J. V.; Fasel, R. *Angew. Chem, Int. Ed.* **2007**, *46*, 1814−1818.
(7) Bobisch, C.; Wagner, Th.; Bannani, A.; Möller, R. *J. Chem. Phys.* **2003**, *119*, 9804−9808.
(8) de Oteyza, D. G.; Garcia-Lastra, J. M.; Corso, M.; Doyle, B. P.; Floreano, L.; Morgante, A.; Wakayama, Y.; Rubio, A.; Ortega, J. E. *Adv. Funct.Mater.* **2009**, *19*, 3567−3573.
(9) Ruiz-Oses, M.; de Oteyza, D. G.; Fernandez-Torrente, I.; Gonzalez-Lakunza, N.; Schmidt-Weber, P. M.; Kampen, T.; Horn, K.; Gourdon, A.; Arnau, A.; Ortega, J. E. *ChemPhysChem.* **2009**, *10*, 896−900.
(10) Krauss, T N.; Barrena, E.; Dosch, H.; Wakayama, Y. *ChemPhysChem.* **2009**, *10*, 2445−2448.
(11) Huang, Y. L.; Chen, W.; Li, H.; Ma, J.; Pflaum, J.; Thye Shen Wee, A. *Small* **2010**, *6*, 70−75.
(12) Wakayama, Y.; de Oteyza, D. G.; Garcia-Lastra, J. M.; Mowbray, D. J. *ACS Nano* **2011**, *5*, 581−589.
(13) Vilmercati, P.; Castellarin-Cudia, C.; Gebauer, R.; Ghosh, P.; Lizzit, S.; Petaccia, L.; Cepek, C.; Larciprete, R.; Verdini, A.; Floreano, L.; et al. *J. Am. Chem. Soc.* **2009**, *131*, 644−652.
(14) de Oteyza, D. G.; Barrena, E.; Dosch, H.; Ortega, E.; Wakayama, Y. *Phys. Chem. Chem. Phys.* **2011**, *13*, 4220−4223.
(15) Llanes-Pallas, A.; Matena, M.; Jung, T.; Prato, M.; Stohr, M.; Bonifazi, D. *Angew. Chem., Int. Ed.* **2008**, *47*, 7726−7730.
(16) Scudiero, L.; Hipps, K. W.; Barlow, D. E. *J. Phys. Chem. B* **2003**, *107*, 2903−2909.
(17) Suto, K.; Yoshimoto, S.; Itaya, K. *J. Am. Chem. Soc.* **2003**, *125*, 14976−14977.
(18) Klauk, H.; Zschieschang, U.; Pflaum, J.; Halik, M. *Nature* **2007**, *445*, 745−748.
(19) de Oteyza, D. G.; Barrena, E.; Osso, J. O.; Sellner, S.; Dosch, H. *Chem. Mater.* **2006**, *18*, 4212−4214.
(20) de Oteyza, D. G.; El-Sayed, A.; Garcia-Lastra, J. M.; Goiri, E.; Krauss, T. N.; Turak, A.; Barrena, E.; Dosch, H.; Zegenhagen, J.; Rubio, A.; et al. *J. Chem. Phys.* **2010**, *133*, 214703-1−214703-6.
(21) France, C. B.; Schroeder, P. G.; Forsythe, J. C.; Parkinson, B. A. *Langmuir* **2003**, *19*, 1274−1281.
(22) Toyoda, K.; Hamada, I.; Lee, K.; Yanagisawa, S.; Morikawa, Y. *J. Chem. Phys.* **2010**, *132*, 13470-1−13470-9.
(23) Peisert, H.; Knupfer, M.; Schwieger, T.; Fuentes, G. G.; Olligs, D.; Fink, J. *J. Appl. Phys.* **2003**, *93*, 9683−9692.
(24) Baldacchini, C.; Allegretti, F.; Gunnella, R.; Betti, M.-G. *Surf. Sci.* **2007**, *601*, 2603−2606.
(25) The PEN molecule has six chemically inequivalent C atoms (Figure 2a). However, XPS and theoretical studies on gas-phase molecules revealed only four different components.[24] We have made use of those same components to fit the PEN spectrum on Au(111), given the similarity to that of gas phase molecules as a result of the weak interactions. F_{16}CuPc has four chemically different carbon atoms.[23] However, only three XPS peaks are distinguishable, as the atoms labeled as C3 and C4 in Figure 2a, bonded to fluorine atoms, have nearly the same binding energy. N and F atoms, have two chemically different sites each, but their chemical environment and consequent binding energies are too similar to be resolved in the XPS spectrum.
(26) Fernandez-Torrente, I.; Franke, K. J.; Pascual, J. I. *J. Phys.: Condens. Matter* **2008**, *20*, 184001.
(27) Stadtmuller, B.; Kroger, I.; Reinert, F.; Kumpf, C. *Phys. Rev. B* **2011**, *83*, 085416-1−085416-10.
(28) de Oteyza, D. G.; Silanes, I.; Ruiz-Oses, M.; Barrena, E.; Doyle, B. P.; Arnau, A.; Dosch, H.; Wakayama, Y.; Ortega, J. E. *Adv. Funct. Mater.* **2009**, *19*, 259−264.
(29) Romaner, L.; Heimel, G.; Bredas, J. L.; Gerlach, A.; Schreiber, F.; Johnson, R. L.; Zegenhagen, J.; Duhm, S.; Koch, N.; Zojer, E. *Phys. Rev. Lett.* **2007**, *99*, 256801-1−256801-4.
(30) The remaining difference between the experimental and theoretical values can be traced back to the fact that the calculations are done on the molecular levels in their ground state, whereas the molecular levels recorded by photoemission spectroscopy are in an excited state. The difference is thus related to the Coulomb interaction of the electron−hole pair produced in the photoemission process.

(31) The F_{16}CuPc HOMO shows a surprisingly low binding energy, being a typical acceptor molecule. A similar scenario, however, was found in previous work on perfluorinated pentacene (ref 32), where only for thicker films, not comparable to this first layer in contact with the metal, larger HOMO binding energies were measured. Previous work on thicker F_{16}CuPc films on Au indeed also reports a much deeper lying HOMO position (ref 33).
(32) Koch, N.; Vollmer, A.; Duhm, S.; Sakamoto, Y.; Suzuki, T. *Adv. Mater.* **2007**, *19*, 112−116.
(33) Shen, C.; Kahn, A. *J. Appl. Phys.* **2001**, *90*, 4549−4554.
(34) The fact that no separate PEN HOMO feature is observed is indicative of an overlap with the F_{16}CuPc HOMO, in agreement with the theory. Because of its narrow width it does not contribute to a broadening of the observed peak. In any case, the overlap being an additional reason to (if anything) broaden the experimental feature, it only supports even more the narrowing of the F_{16}CuPc HOMO.
(35) Horcas, I.; Fernandez, R.; Gomez-Rodriguez, J. M.; Colchero, J.; Gomez-Herrero, J.; Baro, A. M. *Rev. Sci. Instrum.* **2007**, *78*, 013705-1−013705-8.
(36) Cossaro, A.; Floreano, L.; Verdini, A.; Casalis, L.; Morgante, A. *Phys. Rev. Lett.* **2009**, *103*, 119601.
(37) Mortensen, J. J.; Hansen, L. B.; Jacobsen, K. W. *Phys. Rev. B* **2005**, *71*, 035109-1−035109-11.
(38) Enkovaara, J.; Rostgaard, C.; Mortensen, J. J.; Chen, J.; Dułak, M.; Ferrighi, L.; Gavnholt, J.; Glinsvad, C.; Haikola, V.; Hansen, H. A.; et al. *J. Phys.: Condens. Matter* **2010**, *22*, 253202-1−253202-24.
(39) Perdew, J. P.; Zunger, A. *Phys. Rev. B* **1981**, *23*, 5048−5079.
(40) Dion, M.; Rydberg, H.; Schröder, E.; Langreth, D. C.; Lundqvist, B. I. *Phys. Rev. Lett.* **2004**, *92*, 246401-1−2464014.
(41) Román-Pérez, G.; Soler, J. M. *Phys. Rev. Lett.* **2009**, *103*, 096102-1−096102-4.